Environment International 186 (2024) 108597

Contents lists available at ScienceDirect

Environment International

journal homepage: www.elsevier.com/locate/envint

Full length article

Differential impact of diesel exhaust particles on glutamatergic and dopaminergic neurons in *Caenorhabditis elegans*: A neurodegenerative perspective

Nivedita Chatterjee [a,*], Michael González-Durruthy [a], Marta Daniela Costa [b,c], Ana R. Ribeiro [a], Vânia Vilas-Boas [a], Daniela Vilasboas-Campos [b,c], Patrícia Maciel [b,c], Ernesto Alfaro-Moreno [a,*]

[a] NanoSafety Group, International Iberian Nanotechnology Laboratory, 4715-330 Braga, Portugal
[b] Life and Health Sciences Research Institute, School of Medicine, University of Minho, Campus Gualtar, 4710-057 Braga, Portugal
[c] ICVS/3B's - PT Government Associate Laboratory, Braga, Guimaraes, Portugal

ARTICLE INFO

Keywords:
C. elegans
Diesel exhaust particles
Development
Behaviour
Glutamatergic neurodegeneration
Dopaminergic neurodegeneration

ABSTRACT

The growing body of evidence links exposure to particulate matter pollutants with an increased risk of neurodegenerative diseases. In the present study, we investigated whether diesel exhaust particles can induce neurobehavioral alterations associated with neurodegenerative effects on glutamatergic and dopaminergic neurons in *Caenorhabditis elegans* (*C. elegans*). Exposure to DEP at concentrations of 0.167 μg/cm^2 and 1.67 μg/cm^2 resulted in significant developmental delays and altered locomotion behaviour. These effects were accompanied by discernible alterations in the expressions of antioxidant genes *sod-3* and *gst-4* observed in transgenic strains. Behaviour analysis demonstrated a significant reduction in average speed ($p < 0.001$), altered paths, and decreased swimming activities ($p < 0.01$), particularly at mid and high doses. Subsequent assessment of neurodegeneration markers in glutamatergic (DA1240) and dopaminergic (BZ555) transgenic worms revealed notable glutamatergic neuron degeneration at 0.167 μg/cm^2 (~30 % moderate, ~20 % advanced) and 1.67 μg/cm^2 (~28 % moderate, ~24 % advanced, $p < 0.0001$), while dopaminergic neurons exhibited structural deformities (~16 %) without significant degeneration in terms of blebs and breaks. Furthermore, *in silico* docking simulations suggest the presence of an antagonistic competitive inhibition induced by DEP in the evaluated neuro-targets, stronger for the glutamatergic transporter than for the dopaminergic receptor from the comparative binding affinity point of view. The results underscore DEP's distinctive neurodegenerative effects and suggest a link between locomotion defects and glutamatergic neurodegeneration in *C. elegans*, providing insights into environmental health risks assessment.

1. Introduction

According to data from the Global Burden of Disease Study (Collaborators, 2020), outdoor air pollution deaths increased from 2.25 million in 1990 to 4.51 million in 2019 (Hannah Ritchie and Roser, 2022). It can be estimated that Particulate Matter (PM) contributes to about 62 % of deaths related to air pollutants (Fuller et al., 2022). PM is a complex mixture of particles and compounds adsorbed to particles with a wide variety of sources (Li et al., 2023), and some studies indicate that Diesel Exhaust Particles may contribute with about 5–10 % in mass to the total composition of PM in cities (Amador-Muñoz et al., 2011; Park et al., 2018; Zheng et al., 2005). Considering that in cities such as Mexico City and New Delhi, the average concentration for PM_{10} may be in the range of 68–238 μg/m^3 (Jain et al., 2020; Quintana-Belmares et al., 2018a) and for $PM_{2.5}$ in the range of 30–135 μg/m^3 (Quintana-Belmares et al., 2018b; Singh et al., 2021), we can infer that the population in these cities is exposed to concentrations in the range of 3–23 μg/m^3 of diesel particles. For many years, the primary endpoint acknowledged as triggered by PM, including DEP, has been related to cardiopulmonary disease and lung cancer (World Health Organization, 2021; Wichmann, 2007). Notably, there is increasing evidence that PM may be a relevant risk factor for chronic degenerative diseases such as Alzheimer's disease or Parkinson's disease (Krzyzanowski et al., 2023; Peters, 2023; von Mikecz and Schikowski, 2020).

* Corresponding authors.
E-mail addresses: nivedita.chatterjee@inl.int (N. Chatterjee), ernesto.alfaro@inl.int (E. Alfaro-Moreno).

https://doi.org/10.1016/j.envint.2024.108597
Received 29 December 2023; Received in revised form 29 February 2024; Accepted 21 March 2024
Available online 22 March 2024

DEP is a complex mixture containing hundreds of constituents, including a core of elemental carbon, polycyclic-hydrocarbon (PAHs), and nitro-PAHs, among others (Wichmann, 2007). A recent review shows that some PAHs could induce neurotoxic effects (Olasehinde and Olaniran, 2022). The prenatal exposure of mice to DEP, has been demonstrated to elevate anxiety and impair cognition in male offspring (Bolton et al., 2013). This prompts whether neurodegenerative defects are imprinted during early development and only manifest later in life. Another critical avenue for future research is the potential premature onset of neurodegeneration induced by airborne nanoparticles (von Mikecz and Schikowski, 2020).

C. elegans is widely recognized as a powerful model organism in toxicology, biological monitoring, and risk assessment. This recognition is attributed to its short life cycle, ease of maintenance, small and transparent body, comprehensive genomic characterization, detailed cell lineage map, and the availability of reporter and mutant libraries. Additionally, *C. elegans* demonstrates a high level of similarity to mammalian metabolic and neurotransmission pathways, along with a considerable degree of homology with human genes (60 %–80 %), including those associated with diseases (Kaletta and Hengartner, 2006; Leung et al., 2008; von Mikecz and Schikowski, 2020). Despite certain limitations, such as the absence of specific organ equivalents, a smaller immune response system, and notable differences in overall lifespan, *C. elegans* stands out as a sensitive and valuable model for evaluating various exposure modes. This includes acute, chronic, transgenerational, and multi-generation exposures, as well as different routes of exposure, including liquid and solid exposures. It facilitates medium throughput whole organism-level assays with multiple endpoints, such as development, reproduction, feeding, lifespan, and locomotion. This model organism has been instrumental in investigating the effects of pollution from diverse environmental sources, including air pollutants (Ficociello et al., 2020; Liu et al., 2023). However, to date, only three studies have explored the sensitivity of *C. elegans* to DEP (Guo et al., 2014; Wang et al., 2019; Yan et al., 2021).

The nervous system of *C. elegans* hermaphrodites comprises 302 neurons, along with 56 support cells, encompassing nearly all known signalling and neurotransmitter systems found in vertebrates (Bargmann et al., 1993). The well-characterized nature of the nervous system in *C. elegans* allows changes in specific behaviours to be attributed to neuronal circuits and specific genes, guiding further investigations and making *C. elegans* a widely utilized model to unravel how neural circuits and genes contribute to behaviour (Piggott et al., 2011). Consequently, it has been extensively investigated for insights into the aetiology of neurodegenerative diseases, and consistently, it is employed as a tool for screening neuroprotective compounds (von Mikecz and Schikowski, 2020). This organism is well-suited for assessments related to neurotoxicity and neurodegeneration, facilitating the observation of changes in locomotor behaviour, neural architecture, and gene expression (Wang et al., 2023).

This study systematically examined the developmental and neurobehavioural effects of standard DEP in *C. elegans*, employing a long-term, and early-life exposure approach. Recognizing DEP's tendency to precipitate in liquid culture conditions, we utilized both liquid and solid nematode growth medium (NGM) exposure routes for distinct toxicity and behavioural assessments, swimming as well as crawling behaviour. The developmental and neurodegenerative analyses were exclusively conducted on solid NGM media. The exposure commenced at early stages, utilizing age-synchronized bleached eggs or L1 larvae. Most endpoints, including development, neurodegeneration, oxidative stress, were examined at the Day 4 adult stage, with toxicity evaluations extending until Day 7. The impact on neuronal development and neurodegenerations was investigated by observing the effects of DEP on dopaminergic and glutamatergic neurons in transgenic strains. Furthermore, *in silico* molecular docking simulations were conducted, specifically targeting *C. elegans*' glutamatergic transporter and dopaminergic neuronal receptor with DEP mixture components.

2. Materials methods

2.1. DEP characterization and stock preparation

The standardized Diesel Exhaust Particle used in this study were sourced from the US National Institute of Standards and Technology (NIST-SRM2975, obtained from a forklift) (https://tsapps.nist.gov/srmext/certificates/2975.pdf). The comprehensive analysis focused on polycyclic aromatic hydrocarbons (PAHs) and nitro-substituted PAHs (Nitro-PAHs), as detailed in the analysis report. However, no information regarding trace elements and metal contamination was provided in the report. To address this, we conducted trace metal analysis using an ICP-MS instrument (iCAP™ Q, Thermo Fisher Scientific, Waltham, MA) equipped with a Meinhard® (Golden, CO) TQ + quartz concentric nebulizer. Further information on sample preparation can be found in the supplementary materials (section 1.1.1).

To comprehensively understand the DEP, we examined their size, structure, and agglomeration behaviour using transmission electron microscopy (TEM) (JEOL JEM 2100 80–200 kV). Additional details on this analysis are available in the supplementary materials (section 1.1.2).

The DEP were weighed and then dispersed in sterile water at a concentration of 1 mg/mL. These stock suspensions underwent dispersion through sonication for 15 min (Van Den Broucke et al., 2020).

2.2. C. elegans strains

The strains applied in this study - (i) N2, variation Bristol is a *C. elegans* wild-type strain (ii) BZ555 egIs1 [dat-1p:GFP] is a transgenic worm strain used for visualization of dopaminergic neurons, iii) DA1240 adIs1240 [*eat-4*::sGFP + lin-15(+)] X is a transgenic worm strain used for visualization of glutamatergic neurons, iv) CF1553 muIs84 [(pAD76) *sod-3*p::GFP + rol-6(su1006)] is a reporter strain for *sod-3* expression, v) CL2166 dvIs19 [(pAF15)gst-4p::GFP::NLS] III is a reporter strain for *gst-4* expression. All strains were obtained from Caenorhabditis Genetics Centre (CGC).

2.3. Nematode maintenance and exposure to DEP

All *C. elegans* strains were cultured on Nematode Growth Medium (NGM) plates seeded with *Escherichia coli* OP50 strain at 20 °C according to standard methods (Brenner, 1974). The OP50 bacteria were cultured overnight at 37 °C and 180 rpm in Luria Broth (LB) media, then pelleted by centrifugation, inactivated through three cycles of freeze/thawing, frozen at −80 °C, and finally, resuspended in S-medium complete before the assay. In the assay, the appropriate amount of DEP from the stock was first mixed with inactivated (by cycles of freeze/thawing) OP50 suspension (in S-medium with antibiotics). Subsequently, this mixture was applied to NGM plates, corresponding to 0.0167, 0.167, and 1.67 μg/cm^2. Bleached eggs were seeded onto the prepared plates (Day 0) and the exposure continue until Day 4. Unless stated otherwise, the assays were carried out on Day 4 with adult worms.

2.4. Uptake and distribution

The control and DEP treated animals from Day 4 were collected and subjected to the specific washing, fixing steps and the samples were prepared for scanning electronic microscope (SEM) and transmission electron microscope (TEM). The related details can be found in supplementary materials (section 1.3). For SEM approximately 50 worms per condition and for TEM a minimum of 10 animals per conditions with a minimum of 3 sections per animals were analysed.

2.5. Toxicity assessment

The *C. elegans* Bristol strain N2 was used to evaluate the toxicity of

DEP. The NGM-plate based toxicity assay was adapted as previously described (Xiongetal., 2017). Briefly, the eggs, obtained by hypochlorite treatment of adult animals, were left in M9 buffer to hatch overnight at 20 °C to give rise to a population of synchronized L1 larvae. Each well of a 24-well plate containing 500 µL NGM agar was seeded with 20 µL of inactivated OP50 suspension mixed with or without DEP (at concentrations of 0.0167, 0.167, 1.67 µg/cm^2). Either one or three synchronized L1 larvae were added onto each well (Day 1). The plates were incubated at 20 °C and the images of each individual well was captured daily at same time (Olympus SZX16 stereomicroscope with an integrated camera, Olympus SC30) until Day 7. NGM plate was recorded using an Olympus SZX7 stereomicroscope with an integrated camera (Olympus PD72).

The details of the toxicity screening in liquid 96 well plate has been described in the supplementary materials (Section 1.2).

2.6. Growth and development

Approximately fifty age synchronised L1 larvae were exposed to either control or DEP (at concentrations of 0.0167, 0.167, 1.67 µg/cm^2) grown in solid medium. At Day 4 (65 h after hatching), worms were counted according to their life stages in each plate under Olympus SZX16 stereomicroscope with an integrated camera (Olympus PD72). Three independent experiments were conducted each with three technical replicates for each conditions. The worms from each life stage were calculated as % of total worms, and the statistical analysis was performed with two-way ANOVA followed by Tukey's multiple comparisons test.

The control and treated Day 4 adult worms were photographed for growth analysis using an Olympus PD72 digital camera attached to an Olympus SZX16 stereomicroscope. The length of each worm were measured using Image J® software (Vilasboas-Camposet al., 2021). Three independent experiments were conducted each with three technical replicates, approximately 10–15 worms per technical replicates and in total approximately 100 worms were analysed. The statistical analysis was performed with one-way ANOVA followed by Tukey's multiple comparisons test.

2.7. Behaviour analysis

The behavioural analysis was performed at Day 4 of DEP exposure as described in section 2.3.

2.7.1. Swimming behaviour

The WMicrotracker system from InVivo Biosystems (PhylumTech) was employed to assess the locomotion in liquid medium, the swimming activity, of C. elegans. The instrument assesses the combined locomotor activity of all *C. elegans* in liquid-filled multi-well plates by detecting interruptions in infrared micro beams over a specified duration. The animals from DEP treated and control conditions were collected, washed in M9 buffer, and dispensed off in a 96-well plate at approximately fifty animals per well. The activity level was quantified as the count of interruptions observed within 60 min, a calculation performed by the Wmicrotracker software. Three independent experiments were conducted each with six technical replicates and the statistical analysis was performed with one-way ANOVA followed by Tukey's multiple comparisons test.

2.7.2. Locomotion behaviour and speed

The animals were collected, washed and added to unseeded NGM plates, for 30 min. A population of animals in the NGM plate was recorded using an Olympus SZX7 stereomicroscope with an integrated camera (Olympus SC30), for 1 min while moving spontaneously. In each trial and for each condition three videos were recorded and a total of 300–400 animals were scored in at least four independent assays. The videos were processed using the Image J® software and the Wrmtrck plugin (Nussbaum-Krammer et al., 2015; Vilasboas-Campos et al., 2021) and the average crawling speed (mm/sec) was calculated. The statistical analysis were performed with one-way ANOVA followed by Tukey's multiple comparisons test.

2.8. Fluorescence microscopy

Living adult animals (4 days old), both control and exposed, were mounted on 2 % agarose pad with 2.5 mM Levamisole. Fluorescence signal was observed using a Nikon Ni-E Upright Widefield/Fluorescence Microscope with a GFP filter cube (EX 472/30 nm, DM 495 nm, EM 520/35 nm) and a SOLA Lumencor® LED lamp. Images were captured with a Hamamatsu C10600 ORCA-R2 camera at 5X (1.29 µm/px) and 50X (0.13 µm/px) magnification using Nikon TU Plan Fluor objectives. Detection and processing utilized NIS Elements BR v4.30.02 LO software. Bright-field images were also obtained under the same conditions with white-light illumination.). Settings were adjusted for control condition and used equally for treated animals.

2.8.1. Neurodegeneration

The glutamatergic neuronal status was assessed in DA1240 strains in which the green fluorescent protein (GFP) is expressed under the regulation of the glutamatergic transporter, *eat-4*. Dopaminergic neuronal status was analysed in BZ555 transgenic strain in which GFP is expressed under the *dat-1* promoter regulation. Effects on neuronal integrity were examined through quantitative fluorescent imaging of neurodegeneration assays. We adopted a scoring method for glutamatergic neuronal degeneration assessment (Griffin et al., 2018). The DA1240 strain typically exhibits five neurons in the tail region in normal conditions. Any disappearance in the number of neurons was considered indicative of 'neurodegeneration'. Using the reduction in the neuronal count, we applied the standardized scoring approach for assessing degeneration levels, ranging from normal (five neurons) to moderate (four neurons) to advanced (three or less neurons). We assessed dopaminergic neuronal degeneration in the head region of BZ555 transgenic worms, focusing on indicators such as soma shrinkage, blebs and breaks in dendrites as previously described (Markovich et al., 2022). A one-hour treatment with 25 mM 6-hydroxydopamine (6-OHDA) in 5 mM ascorbic acid served as the positive control for dopaminergic neurodegeneration. Independent experiments were conducted with Day-4 adult animals for five times and least twenty animals were analysed per treatment in each experiment and the statistical analysis were conducted with two-way ANOVA followed by Tukey's multiple comparisons test.

2.8.2. Assessment of antioxidant response

The antioxidant response was assessed in in *gst-4*, *sod-3* genes using reporter strains. In the CL2166 strain, the fluorescent protein (GFP) indicated the transcription level of glutathione transferase (*gst-4*) and in the CF1553 strain, GFP indicated the transcription level of superoxide dismutase (*sod-3*).. The quantitative fluorescence intensity of each worm, measured using Image J® software (Vilasboas-Camposet al., 2021), divided by the total area (in CL2166) or by the head-pharynx region of respective animals (in CF1553) and normalized to the mean of the control worms. Independent experiments were done four times and least twenty animals were analysed per treatment in each experiment and the statistical analysis were carried out with one-way ANOVA followed by Tukey's multiple comparisons test.

2.9. In silico methodology

The methodology had the stages that follow: (i) Performing 3D-homology modelling and crystallographic validation of the neuro-target receptors from *C. elegans* (ex., eat-4_Ce, dop-1_Ce), (ii) Performing binding-sites prediction of the neuro-targets from *C. elegans* (ex., eat-4_Ce, dop-1_Ce); (iii) Performing structure-based virtual screening on

DEP compounds with eat-4_Ce, dop-1_Ce. The details of each three steps can be found in supplementary materials (section 1.4). It is important to note that, in general terms, mechanistic studies of interactions involving mixture of compounds still pose a significant challenge, and certain *in silico* limitations are inherent when increasing the complexity of the system under investigation on *in silico* modeling neuro-nanointeractions of complex nano-mixtures of DEP at the molecular levels (toxicodynamics). In this context, strategies for addressing these potential limitations and challenges are outlined in the supplementary material (Table S1) regarding each of the step of the *in silico* methodology and also by including crystallographic quality validation based on Ramachandran plot (Fig. S1).

2.10. Statistical analysis

The statistical analysis and generation of graphs for all endpoints were performed using GraphPad Prism 10.0.2 software. Replication details and corresponding statistical analyses, including post-hoc methods, were specified for each endpoint analysis.

3. Results and discussion

3.1. DEP particles

The spherical DEP particle with a primary size of 39 nm surface were

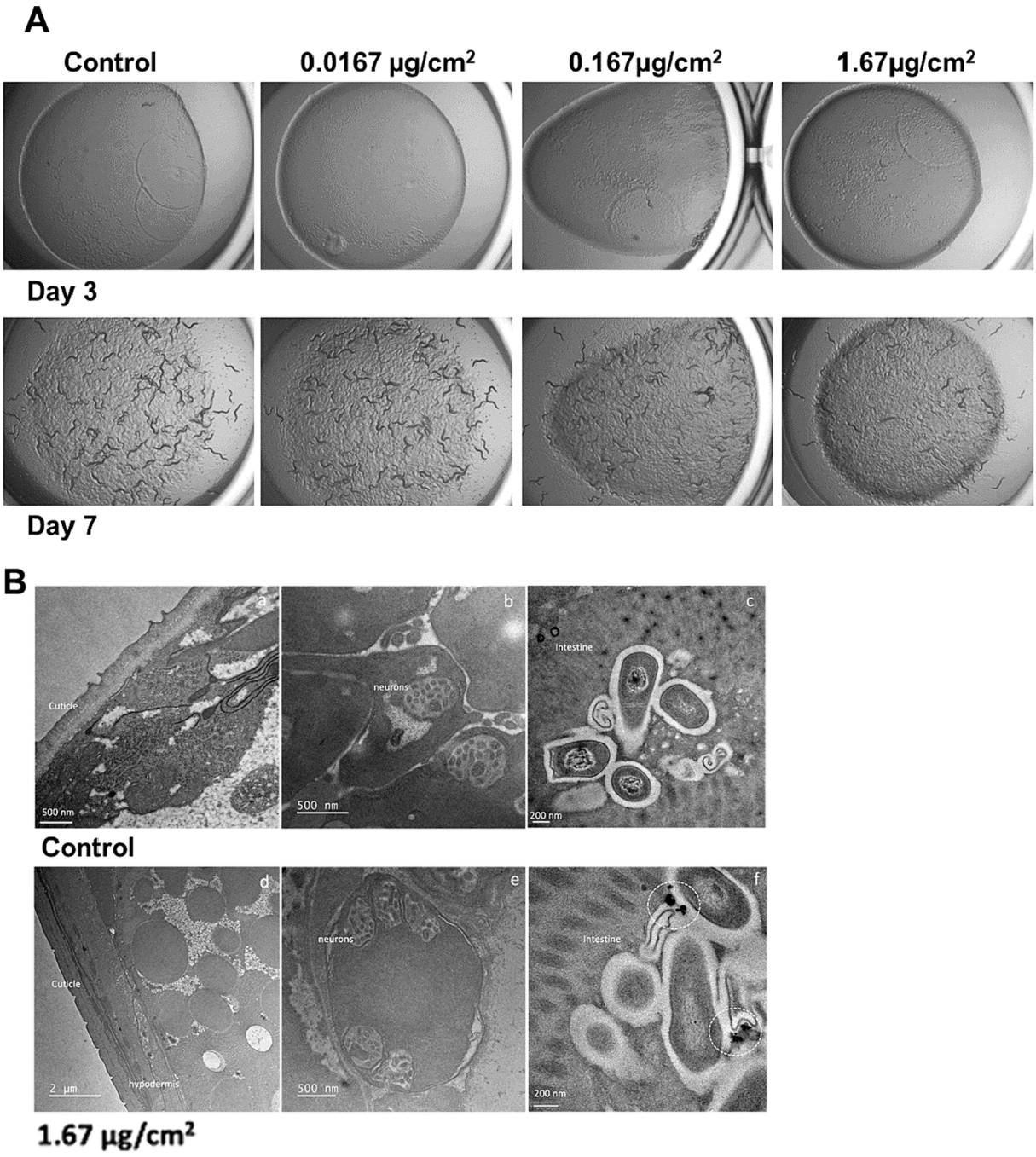

Fig. 1. The toxicity, uptake and distribution of diesel exhaust particles on *C.elegans*. **A.** The food-clearance-based toxicity assessment of DEP on NGM-plate. Exposures were performed with single age-synchronized L1 larva per well for seven days at control and various doses of DEP in a 24-well plate format. Images were taken each day until Day 7. The respective well images of Day 3 and Day 7 were presented. **B.** The transmission electron microscopic (TEM) micrograph of *C. elegans* longitudinal cuts in control conditions (a, b, c) and exposed to higher concentrations of DEPs (d, e, f). Dotted circles indicate particles' aggregates.

evident in the TEM micrograph of the DEP (Fig. S2). According to the results of trace metal analysis presented in Table S2, all metals were found to be in negligible concentrations compared to reported exposure levels to induce neurotoxicity.

3.2. Toxicity of DEP

In general, the food-clearance-based assays in both liquid and solid NGM exposure methods revealed that DEP has no critical effects on the survival of *C. elegans*. On the final day (Day 7) of liquid assay, statistically significant differences in half-life (represented by the K constant) were observed only at the highest dose (100 μg/mL) compared to the control group ($p = 0.019$) (Fig. S3A). The liquid exposure conditions may not be the ideal medium for particles, including DEP, due to the inconsistent stability of particle suspension in the liquid medium. This initial screening test provides an idea about the toxicity effects, further

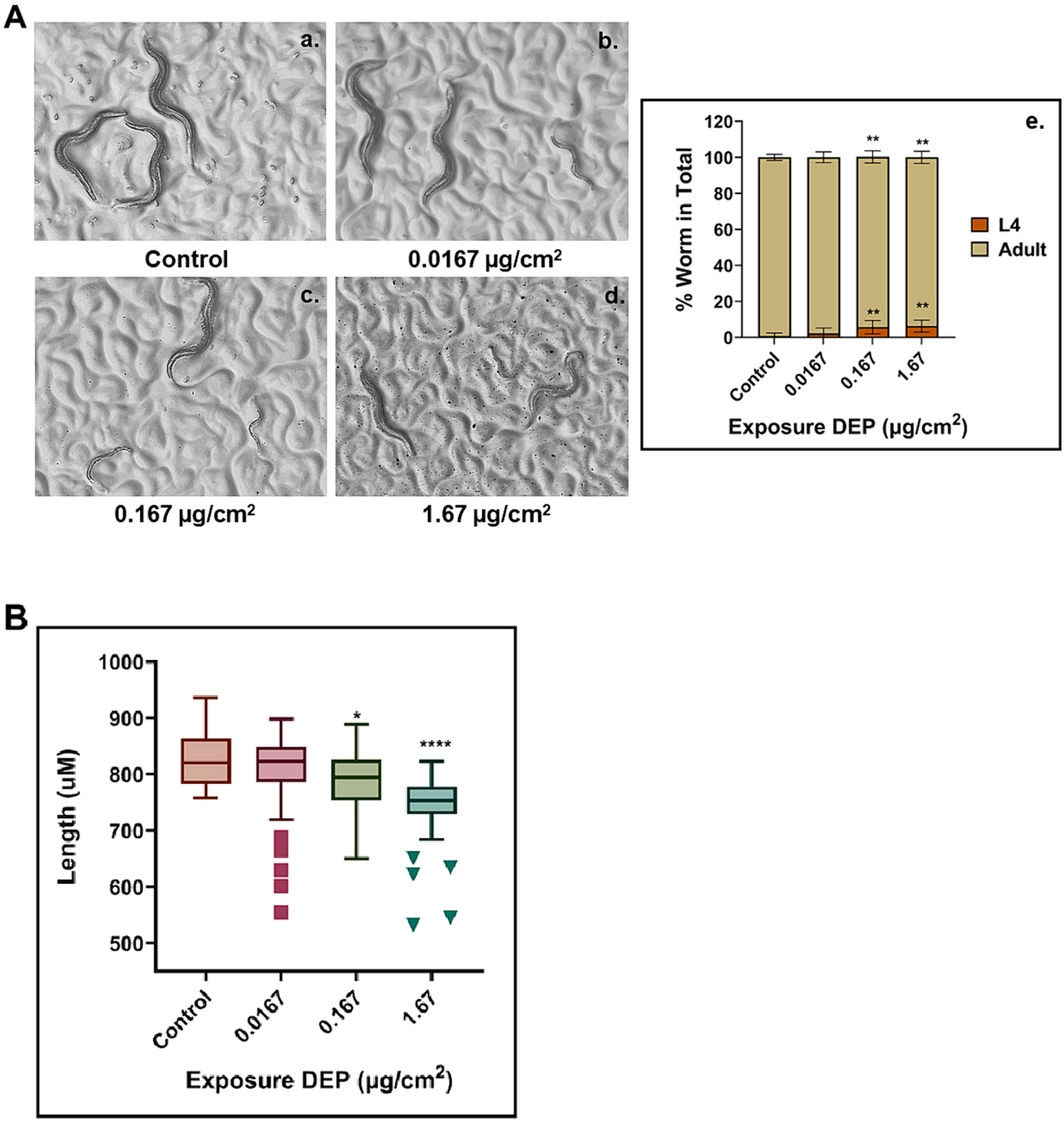

Fig. 2. Effects of diesel exhaust particles on development and growth of *C.elegans*. **A.** Worms at different life stages with representative images from each exposure conditions, with and without DEP – a. control, b. 0.0167 μg/cm^2, c. 0.167 μg/cm^2, d. 1.67 μg/cm^2 and e. graphical presentation of the percentage of L4 larva and adult worms in total worm population. Exposures were performed from age synchronized L1 (Day 1) to Day 4 (at ~65 h after hatching) at various doses of DEP on solid NGM plates. Data represent Mean ± SD, ** $p \leq 0.005$. **B.** Body length of worms at Day 4 after exposure to DEP. Exposures were performed from bleached egg until Day 4 at various doses (control, 0.0167, 0.167, 1.67 μg/cm2) on solid NGM plates. Data presented as Box-and-Whisker Plot with Tukey-Style Whiskers, * $p \leq 0.05$, ** $p \leq 0.005$; **** $p < 0.0001$.

confirmed with the solid (NGM-based) screening mode. Similar to the liquid exposure mode, solid exposure is also based on a food clearance assay, where fewer animals result in more remaining food until Day 7. Adverse impacts of DEP were evident when exposing either a single worm (Fig. 1A) or three worms (Fig. S2B) per well. Marked differences in food clearance were evident from the control to the highest exposure dose of DEP (1.67 μg/cm^2). DEP, between the doses of 0.0167–1.67 μg/cm^2, possibly does not cause severe harm to the survival of the animals but negatively impacts their development and fecundity status (Wang et al., 2019). Consistent with our study, the induction of lethality was not observed in either acute or prolonged exposure to airborne particulate matter (PM) $PM_{2.5}$ from coal combustion (Sun et al., 2015), traffic-related $PM_{2.5}$ (Chung et al., 2020; Zhao et al., 2014), field collected fine $PM_{2.5}$ (Chung et al., 2019) and field-collected water soluble $PM_{2.5}$ (Zhang et al., 2023).

3.3. Uptake and the distribution of DEP particles

As expected, control group worms lacked DEP structures (Fig. 1B. a, b, c). In exposed conditions (1.67 μg/cm^2), DEP were mainly found in *the C. elegans* intestinal lumen, taken up during oral feeding (Fig. 1B, d, e, f). No DEP were observed inside gut cells, and they remained within the intestinal lumen, separated from microvilli. These DEP did not harm tissues and were confined to the intestine. Translocation and distribution to other tissues, such as neurons, were also not visible (Fig. 1B. d). Moreover, no significant changes in cuticle morphology, discerned by SEM analysis, were observed with varying DEP concentrations (Fig. S4). In a similar line of evidence, accumulation of DEP only in the intestinal lumen of *C.elegans* was also reported (Yan et al., 2021). The exclusive presence of DEP accumulation within the intestinal lumen suggests a potential restriction in DEP excretion, highlighting that the primary exposure route is likely through feeding.

3.4. Impacts of DEP on growth and development

In our investigation of the effects of DEP on growth and development, as evidenced by solid NGM toxicity tests, we observed developmental delays caused by DEP exposure. At Day 4 (~65 h after hatching), when all animals should have reached the adult stage under normal conditions, we observed a mixed population of adults and L4 larval stages in DEP-treated plates (Fig. 2A). Regarding growth, as measured by body length, discernible differences were observed in DEP-treated conditions at Day 4 life stages (Fig. 2B). The highest exposure concentration of DEP (1.67 μg/cm^2) resulted in approximately a 12 % reduction in growth by Day 4. Our approach included two distinct assays: one focused on identifying and quantifying specific life stages of animals, and the other utilized a growth assay measuring body length. Notably, most prior studies on airborne PM, particularly DEP, primarily assessed growth and development by examining 'body length'. Previous studies using *C. elegans* and mammalian models suggest that airborne particulate matter, including DEP and toluene, exposure can lead to growth retardation, evident as decreased body length (Haghani et al., 2019; Liu et al., 2023; Caceres Quijano et al., 2022; Soares et al., 2020; Liu et al., 2023 Ema et al., 2013). Similarly, a transgenerational study with traffic-related PM2.5, containing components like DEP, revealed shortened growth in both exposed parents and their offspring (Zhao et al., 2014). These findings suggest potential mechanisms like reduced food intake and nutrient absorption due to DEP accumulation in the intestines (Liu et al., 2023), and potentially additional factors like DNA damage, disrupted cell cycles, and increased germline cell apoptosis (Soares et al., 2020). While our current study did not explicitly investigate these mechanisms, further exploration of the underlying causes of developmental delays is warranted, which will be a focus of our future work.

3.5. Behavioural alterations in DEP-treated animals

Locomotion serves as the foundation for most, if not all, *C. elegans* behaviours, encompassing sensory, social, mating, sleep, drug-dependent behaviours, and learning and memory, with these behaviours being, to varying degrees, manifested at the locomotion level (Piggott et al., 2011). Significant behavioural changes were evident in DEP-exposed conditions. Overall, a significant decline in swimming activities ($p < 0.005$) (Fig. 3A), reduced average speed ($p < 0.0001$), and shrinkage in crawling paths (Fig. 3B) was observed in response to DEP exposure at concentrations ranging from 0.167 μg/cm^2 to 1.67 μg/cm^2. A substantial dose-dependency was manifested in average speed, particularly between 0.167 μg/cm^2 and 1.67 μg/cm^2 (Fig. 3B). Spontaneous locomotor disorders, such as head thrashing and body bending frequency, were observed not only in the DEP-exposed generation (F0) of the *C. elegans* model but also persisted in the directly unexposed next generation (F1), indicating the potential impact of DEP on transgenerational neuronal developmental processes (Yan et al., 2021). Consistent with our findings, previous research demonstrates DEP-induced behavioural changes. In mice, in utero exposure to DEP (171 μg/m3) decreased spontaneous locomotor activity in male offspring (Suzuki et al., 2010). Conversely, high-level exposure in mice (1000 μg/m^3) increased locomotor activity and repetitive behaviors (Thirtamara Rajamani et al., 2013). Similarly, *C. elegans* studies using airborne particulate matter (various sources and components) consistently showed reduced locomotion behaviours (head thrash, body bend) (Liu et al., 2023; Zhang et al., 2023; Sun et al., 2015; Chung et al., 2019; Chung et al., 2020). Notably, a transgenerational study with traffic-related PM2.5, containing components like DEP, revealed reduced locomotion behaviour in both the exposed parents and unexposed their offspring (Zhao et al., 2014). (10–100 μg/mL) (Zhao et al., 2014). Lastly, airborne toluene exposure intriguingly induced dose-dependent reductions in mean velocity and swimming movement in *C. elegans*, further supporting our observations (Soares et al., 2020).

Behavioural assays offer valuable insights into neuronal function (Liu et al., 2023). While they enable rapid screening, pinpointing specific neuronal disruptions often requires deeper investigation (Smith et al., 2019). In *C. elegans*, locomotion and motor functions are primarily controlled by dopaminergic, glutamatergic, cholinergic, and GABAergic neurons (Li et al., 2017; Yu et al., 2022). We focus on examining dopaminergic and glutamatergic neurons due to their role in locomotion and implications in Parkinson's (Hughes et al., 2022) and Alzheimer's diseases (Griffin et al., 2019), respectively. For assessing neurodegeneration, we prioritize analysing morphology in transgenic strains, as it offers greater reliability compared to fluorescence intensity measurements (Smith et al., 2019). While methods for quantifying dopaminergic neurodegeneration (using BZ555 or BY200 strains) are established in studies of airborne particulate matter toxicity, our quantification of glutamatergic neurodegeneration (in the DA1240 strain) by analysing posterior glutamatergic neurons introduces a novel approach specifically for environmental pollutant toxicity studies.

3.6. Impact of DEP on neurodegeneration

3.6.1. Glutamatergic neurodegeneration

In the *C. elegans* DA1240 strains the fluorescent protein (GFP) is expressed under the regulation of the, *eat-4*, promoter, specific of some glutamatergic neurons. Effects of DEP on glutamatergic neuronal integrity were examined through quantitative fluorescent imaging of posterior glutamatergic neurons. In worms, the glutamatergic neurons are comprised of 16 different anatomical types, a total of 34 cells (Mano et al., 2007) while the five neurons in the posterior glutamatergic circuitry, being anatomically distinct, readily observable, and quantifiable, provide a convenient output for scoring neurodegeneration, exhibiting progressive degeneration early in life (Griffin et al., 2018). To the best of our knowledge, this is the first report on morphological-based

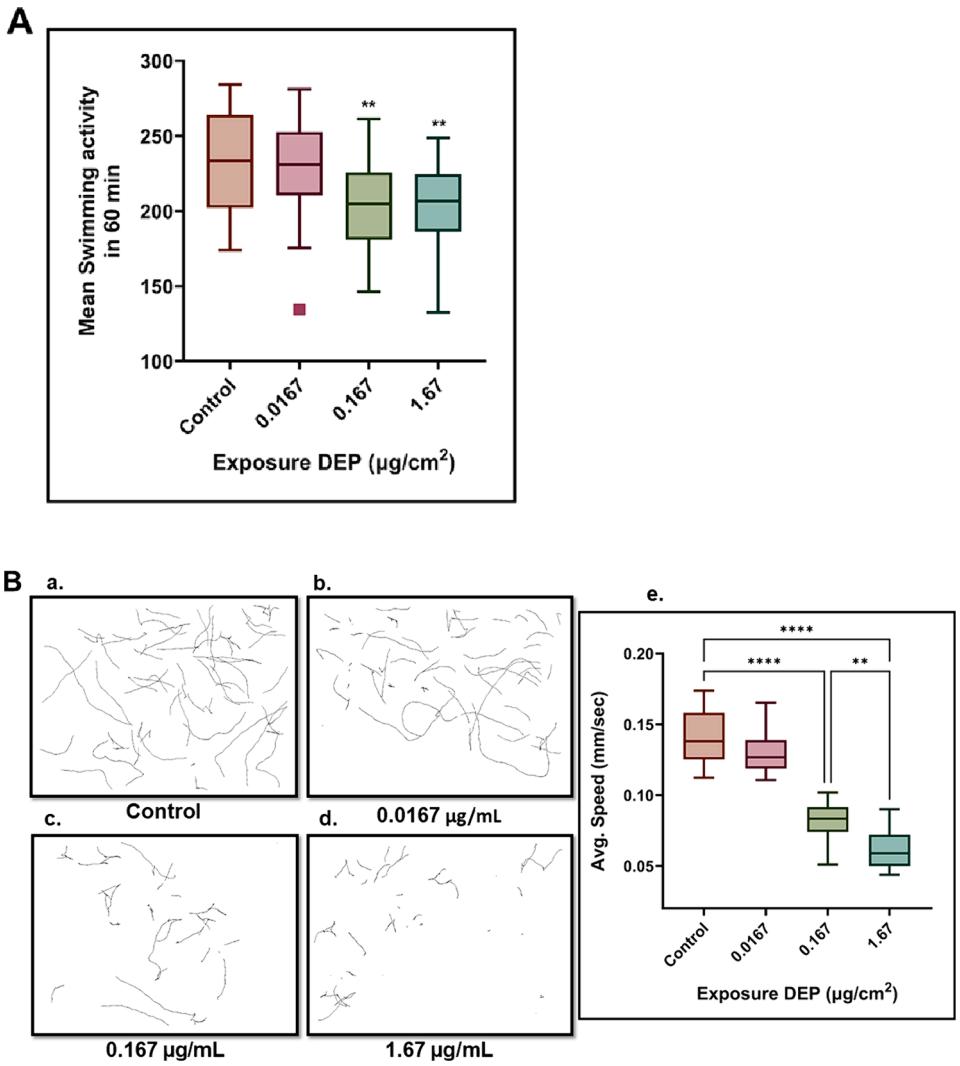

Fig. 3. Effects of diesel exhaust particles on *C.elegans* behaviour. **A.** Alterations in swimming behaviour. Exposures were performed from the bleached egg until Day 4 on solid NGM plates; after that, collected worms were dispensed in S-buffer and analysed in WMicrotracker system. Data presented as Box-and-Whisker Plot with Tukey-Style Whiskers, ** $p \leq 0.005$; **** $p < 0.0001$. **B.** Locomotion, with the representative images of the crawling path from reach exposure conditions – a. control, b. 0.0167 µg/cm^2, c. 0.167 µg/cm^2, d. 1.67 µg/cm^2 and e. average speed (mm/second). Exposures were performed from bleached egg until Day 4 on solid NGM plates, and after that collected worms were added onto fresh NGM plates, followed by the acquisition is videos and analysis in Image J with 'WormTacker' plugin. Data presented as Box-and-Whisker Plot with Tukey-Style Whiskers, ** $p \leq 0.005$; **** $p < 0.0001$.

quantitative scoring for posterior glutamatergic neuronal status in *C. elegans* in particles' toxicology. Our findings revealed significant degeneration in glutamatergic neurons due to DEP exposure. At a concentration of 0.167 µg/cm^2, approximately 30 % exhibited moderate degeneration, and 20 % showed advanced degeneration. At a concentration of 1.67 µg/cm^2, approximately 28 % displayed moderate degeneration, and 24 % showed advanced degeneration ($p < 0.0001$) (Fig. 4A). However, the dose dependency, particularly between the concentrations of 0.167 and 1.67 µg/cm^2, was not significantly different. The representative images from each exposure condition were presented as Fig. S5A. While our research did not specifically centre on an Alzheimer's disease model, our findings regarding glutamatergic neuronal loss coincide with the outcomes seen in amyloid-$\beta_{1\text{-}42}$ (Aβ) peptide-induced effects on glutamatergic neurodegeneration (Griffin et al., 2019; Griffin et al., 2018). Notably, the presence of airborne nanoparticles intensified the aggregation of Aβ in the body wall muscle cells of *C. elegans* (Garcia Manriquez et al., 2023; von Mikecz and Schikowski, 2020).

3.6.2. Dopaminergic neurodegeneration

The changes in the morphological patterns of dopamine neurons were discerned through the application of *dat-1*:GFP labelling in the transgenic strain BZ555 nematodes. There are four bilaterally symmetric pairs of dopamine neurons, comprising three pairs located within the head—specifically, two pairs of cephalic sensillum (CEP) neurons and one pair of anterior deirids (ADE) neurons. One pair of dopamine neurons is also situated in the mid-body region, specifically as posterior deirids (PDE) neurons. No significant degeneration was observed, such as blebs or dendrites' breakage, as evidenced in the positive control 25 mM 6-hydroxydopamine (6-OHDA). The structural deformities and morphological deviation ($p \leq 0.05$) were observed in CEP neurons which comprise up to ~16 to 17 % at the high exposure concentrations (0.167 and 1.67 µg/cm^2) (Fig. 4B). However, there are almost no difference in between the dose of 0.167 µg/cm^2 vs 1.67 µg/cm^2. The representative images from each exposure dose were presented as Fig. S5B. In particular, a previous study with DEP exposure documented a reduction in dopamine transporter expression (*dat-1*) and loss of CEP neurons in BZ555 strains (Yan et al., 2021). The results are partially in line of agreement with our study that there is no alterations in ADE,

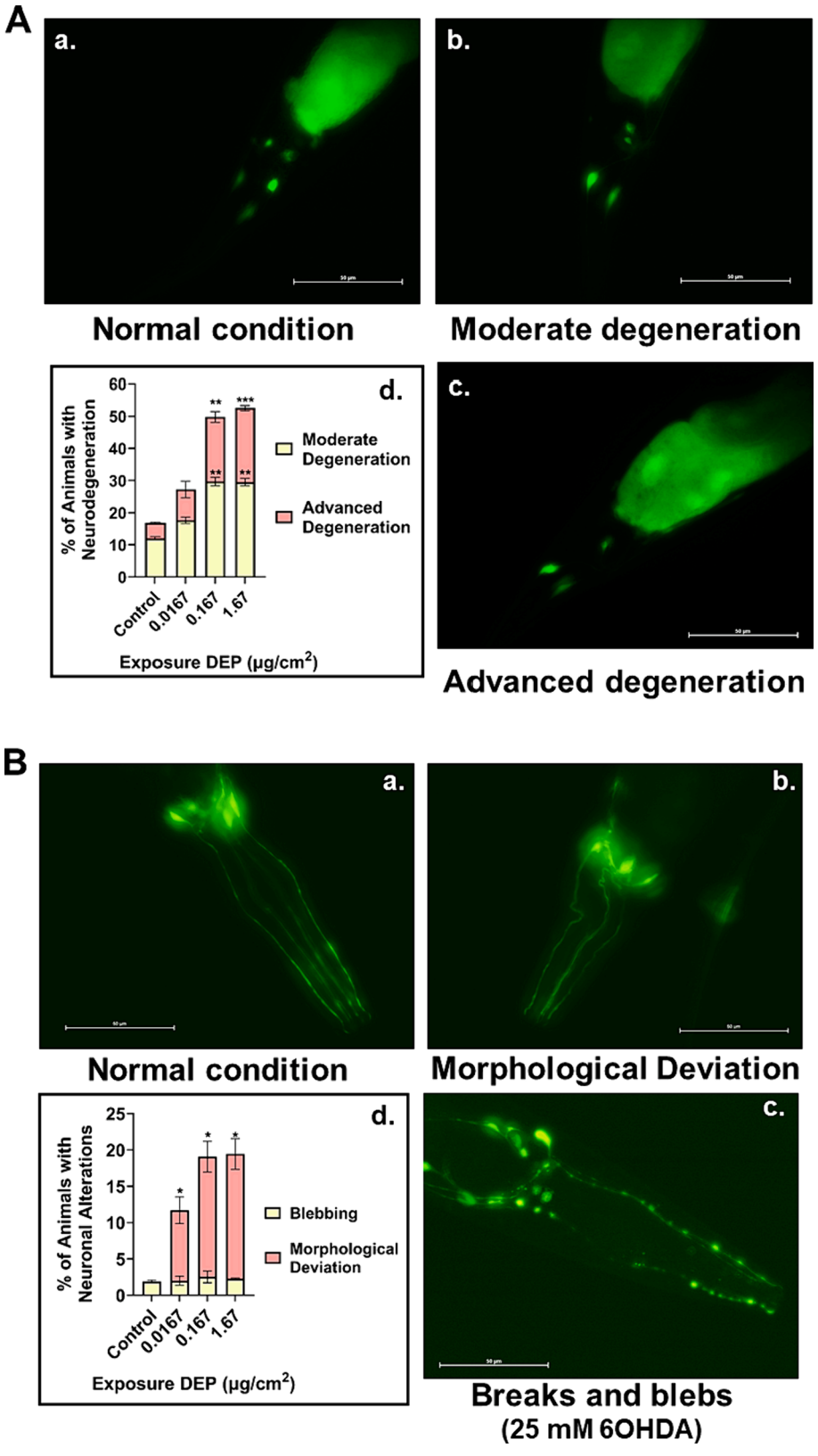

Fig. 4. Effects of diesel exhaust particles (DEP) on *C.elegans* neurodegeneration. Exposures were performed from bleached eggs (Day 0) to Day 4 on solid NGM plates with and without DEP. At Day 4, the live worms were observed under a fluorescence microscope. **A.** Glutamatergic neurodegeneration in DA1240 strain. The analysis and scoring was performed on the five posterior glutamatergic neurons. Representative images of (a.) normal condition presence of all five posterior neurons, (b.) moderate neurodegeneration, i.e., presence of four posterior neurons, (c.) advanced neurodegeneration, i.e., presence of three or fewer posterior neurons, (d.) the graphical presentation of quantitative analysis of moderate and advanced degenerations. **B.** Dopaminergic neurodegeneration in BZ555 strain. The analysis and scoring were performed in the head regions (AED and CEP neurons). The representative images depicting (a.) normal conditions, (b.) deformations, and (c.) the

positive control with blebbing and breaks (25 mM 6OHDA), (d.) the graphical presentation of quantitative analysis of blebbing and deformation of CEP neurons. Image scale bar 50 μm. Data are presented as Mean ± SD with a stacked bar; * $p \leq 0.05$; ** $p \leq 0.005$; *** $p \leq 0.001$.

while significant changes were evident in CEP neuronal regions. The main exception was the intensity of damages in CEP regions reported as 'neuronal loss,' while we found mainly the deviation of shape in dendrites and soma, not particular 'neuronal loss'. The differences may be caused due to the exposure mode. This particular strain has been applied to evaluate dopaminergic neuronal loss in various particles and nanomaterials. For instance, dendritic beading was observed in single PDE neurons due to tire component exposure (Limke et al., 2023).

Our findings illustrate that exposure to DEP induces neurotoxicity in both dopaminergic and glutamatergic neurons, potentially influencing alterations in locomotion.. Previous research on the functional mapping of neuronal circuits in worms has revealed a dual mode of motor

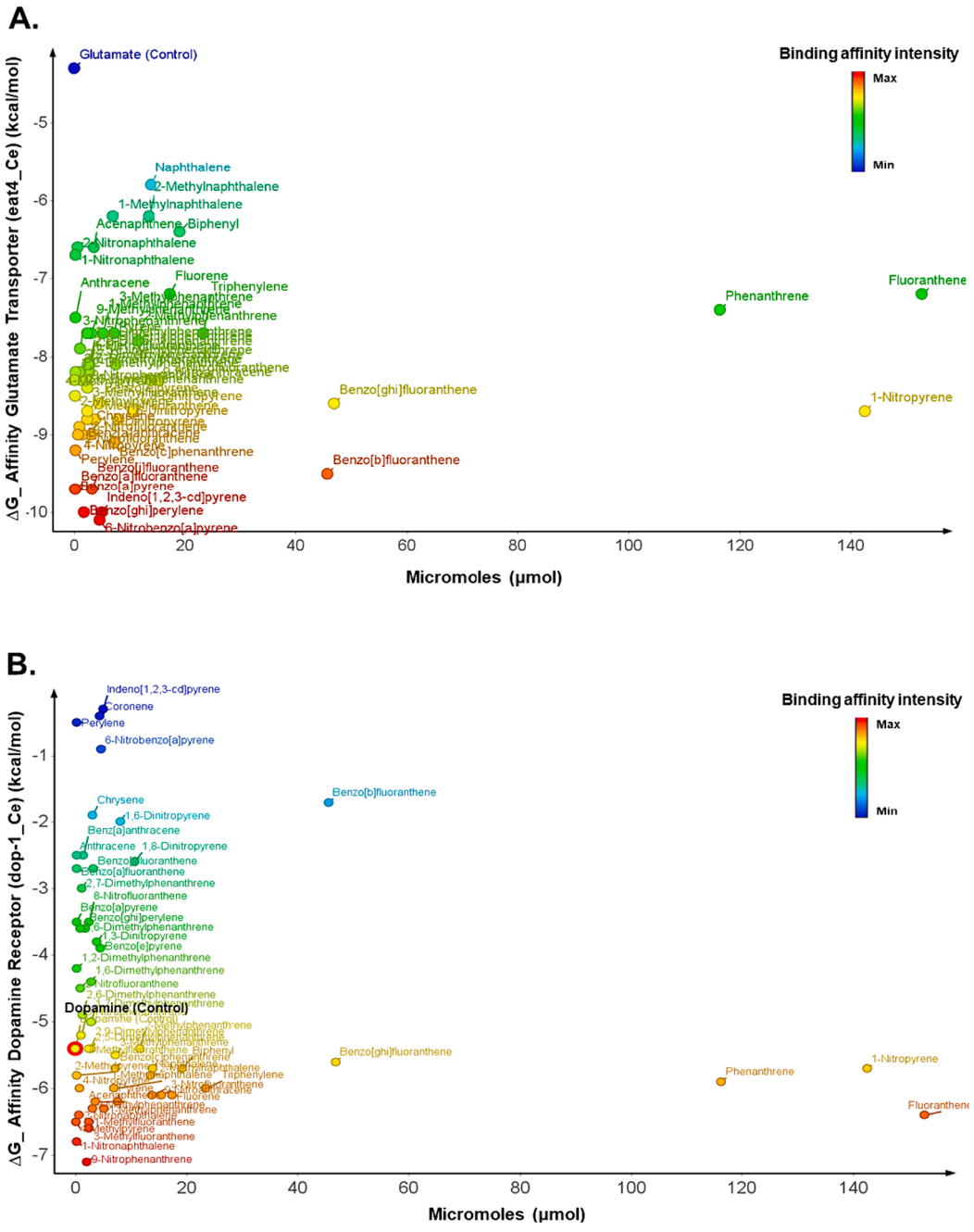

Fig. 5. The 2D-scatter plots illustrating *in silico* results from structure-based docking virtual screening for all compounds within the DEP complex mixture interacting with the binding sites of *C. elegans* glutamatergic transporter (eat-4_Ce) and dopaminergic receptor (dop-1_Ce). The x-axis represents concentrations (μmol) of each DEP component, while the y-axis represents interaction binding affinity (ΔG in kcal/mol). Clusters of structurally similar DEP chemical components with comparable interaction affinity values are color-coded, allowing for easy comparison. The colour intensity bar on the right side ranges from minimum to maximum (red), aiding affinity comparisons. **A.** The 2D scatter plot of *C. elegans* glutamatergic transporter (eat-4_Ce) and the plot include the binding affinity of the glutamate neurotransmitter as a reference control of simulation for comparison purposes. **B.** The 2D-scatter plot of *C. elegans* for the dopaminergic receptor (dop-1_Ce) and the plot includes the binding affinity of the dopamine neurotransmitter as a reference control of simulation for comparison purposes.

initiation control, where disinhibitory and stimulatory circuits work together to promote the initiation of backward movement. This process relies on glutamatergic transmission but involves distinct glutamate target structures (Piggott et al., 2011). Consequently, the observed severe DEP-induced glutamatergic neuronal loss may be linked to abnormal locomotion behaviour, particularly in crawling on NGM plates, associated with the functional motor circuit.

Similar to mammals, in *C. elegans*, glutamatergic neurotransmission plays a crucial role in ensuring critical biochemical functions such as memory, cognition, and learning processes, and the involvement of glutamate transporters, exemplified by eat-4_Ce, is particularly significant (Mano et al., 2007). On the other hand, dopaminergic neurotransmission encompasses both dopaminergic D1-like (dop-1_Ce) and D-2-like receptors (dop-2_Ce and dop-3_Ce) (Felton and Johnson, 2014). In parallel with our experimental studies utilizing transgenic strains to visualize glutamatergic and dopaminergic neurons, we employed an *in silico* molecular docking simulation method to examine the DEP binding interactions in both the glutamatergic transporter (eat-4_Ce) and dopaminergic receptor (dop-1_Ce).

3.7. In silico molecular docking analysis of neuro-receptor with DEP mixture compounds

In our *in silico* molecular docking simulation, we observed that all compounds within the DEP mixture exhibit a higher affinity (ΔG values ranging from −5.8 kcal/mol to −10.1 kcal/mol) for the glutamatergic transporter (eat-4_Ce transporter) compared to glutamate (ΔG = -4.3 kcal/mol) itself (Fig. 5A). Conversely, their affinity for the dopaminergic receptor (dop-1_Ce receptor) generally falls below that of dopamine (ΔG = -5.4 kcal/mol) (Fig. 5B). Structurally, both PAHs-DEP and Nitro-PAHs-DEP, the evaluated DEP, display high lipophilic-based aromaticity properties, indicating their potential to traverse biological barriers and impact both glutamatergic and dopaminergic neuro-targets in *C. elegans*. Our results strongly suggest that the compounds in the DEP mixture can spontaneously interact with eat-4_Ce and dop-1_Ce targets in a thermodynamically stable manner. Specifically, the docking complexes formed between DEP and eat-4_Ce transporter exhibit stronger interactions than the reference control (glutamate with a ΔG = −4.3 kcal/mol), suggesting a potential inhibitory effect on the physiological binding of the glutamate neurotransmitter. The theoretical results also suggest that the whole complex mixture of DEP could occupy the same biophysical environment as the glutamate neurotransmitter in the native eat-4_Ce binding site (Guseynov et al., 2019) (Fig. S6A). On the other hand, our findings indicate that certain compounds in the DEP mixture could strongly interact with the dop-1_Ce receptor, potentially blocking the excitatory action of dopamine, while the majority of compounds exhibit a lower affinity for the dop-1_Ce receptor than reference control (dopamine with a ΔG = −5.4 kcal/mol). Moreover, the theoretical results suggest that most compounds in the DEP complex mixture, particularly those with higher ΔG than dopamine (ΔG = −5.4 cal/mol), may not occupy the same biophysical environment as the dopamine neurotransmitter in the native dop-1_Ce binding site (Fig. S6B). However, it is important to note that all these compounds exhibit negative ΔG (kcal/mol) < 0 values and consequently present an overall spontaneous binding process in the dop-1_Ce receptor. While all DEP components are lipophilic, their complex interactions associated with lipophilic properties pose challenges for understanding their toxicokinetics (TK) and toxicodynamics (TD). In this context, we have modelled the relationship between the DEP component's lipophilicity and their corresponding binding affinity (ΔG) values in both *C. elegans* neuro-targets (eat-4_Ce and dop-1_Ce). Then, with the aim of going deeper into this aspect, a complex network analysis was performed. Please, find the details as part of the supplementary materials (Fig. S7A and B).

The findings from our *in silico* molecular docking simulations align seamlessly with our experimental neurodegenerative data, revealing a heightened vulnerability of glutamatergic neurons compared to dopaminergic neurons. This heightened sensitivity may stem from the competitive inhibition mechanism disrupting the excitatory response in *C. elegans* glutamatergic synapses. As suggested by the *in silico* results, the potential dysfunction of glutamate transporters could further contribute to the observed impact on neuronal viability (Armada-Moreira et al., 2020).

3.8. Induction of antioxidant enzyme expression by DEP exposure

In order to assess the induction of antioxidant and detoxification responses, we examined the expressions of two prominent antioxidant enzymes, superoxide dismutase (SOD-3) and glutathione S-transferase (GST-4), using transgenic reporter strains (CF1553 and CL2166, respectively). In the CF1553 strains, GFP is expressed under the *sod-3* promoter, while in the CL2166 strains, GFP is expressed under the *gst-4* promoter. The chronic developmental exposure to DEP resulted in a 1.2 to 1.4-fold increase in *sod-3* expressions, displaying a distinct lack of clear dose dependency (Fig. 6A). The most notable ($p < 0.05$) upregulation of *sod-3* was observed at the mid-dose of 0.167 μg/cm^2. Interestingly, *gst-4* expressions exhibited a unique pattern, with the lowest DEP dose (0.0167 μg/cm^2) showing a more than 2-fold increase ($p < 0.0001$). In comparison, the highest dose (1.67 μg/cm^2) caused an approximately 1.6-fold decrease ($p < 0.003$) in *gst-4* expressions compared to control (Fig. 6B). A clear and consistent dose-dependent reduction among the exposed conditions was evident in the case of *gst-4* expression.

The strong association between air pollution and oxidative stress is well-established. Our recent review provides a comprehensive analysis of how oxidative stress plays a central role in regulating physiological to toxicological responses induced by exposure to particulate matter (Vilas-Boas et al., 2024). A 24-hour exposure at the L4 stage revealed a significant elevation in both gst-4 and sod-3 expressions with increasing concentrations of $PM_{2.5}$ (Zhao et al., 2019). Reactive oxygen species (ROS), particularly singlet oxygen ($^1O_2$), which is a potential transformation product of superoxide ($\cdot O_2^-$), significantly increased in *C. elegans* upon exposure to DEP (Guo et al., 2014). This observation aligns with our findings of increased *sod-3* expressions, as *sod-3* is the enzyme responsible for scavenging superoxide but contradicts the findings of others, as no significant alterations in *sod-3* expression were found in the DEP-exposed transgenic strain CF1553 (Yan et al., 2021). This disparity may stem from the differences in exposure modes and worm life stages.

Furthermore, airborne nano-sized PM originating from traffic emissions exhibited dose-dependent increases in *gst-4* expression at both L1 and L4 stages (Haghani et al., 2019). Intriguingly, a similar pattern to our study of *gst-4* expressions, characterized by induction in lower concentrations but reduction in higher concentrations, was observed in bisphenol A-exposed worms (Wang et al., 2023). We hypothesize that DEP induces an increase in antioxidant enzyme expressions as a defence mechanism at lower doses; however, expressions decrease at higher concentrations, potentially due to the depleted antioxidant defence capacity, particularly within the glutathione pool.

The observed toxic effects on development, behaviour, and neurodegeneration are likely associated with the PAHs mixture in DEP, as indicated by prior studies (Olasehinde and Olaniran, 2022; Soares et al., 2020; Yang et al., 2023), rather than trace metals, which were below the threshold level in the DEP mixture (Table S1). Although DEP translocation was absent in neurons and other organs, except the intestine (Fig. 1B), the presence of PAHs suggests potential harm to the neuronal system through diffusion, as seen with other volatile odorants (Bargmann et al., 1993). A recurrent question related to this type of studies is whether the range of analysed doses/concentrations, are relevant to real life human exposure. In the case of this study, the question is even harder to address, considering that *C. elegans* does not have lungs, and therefore the exposure is by contact and ingestion. However, we could

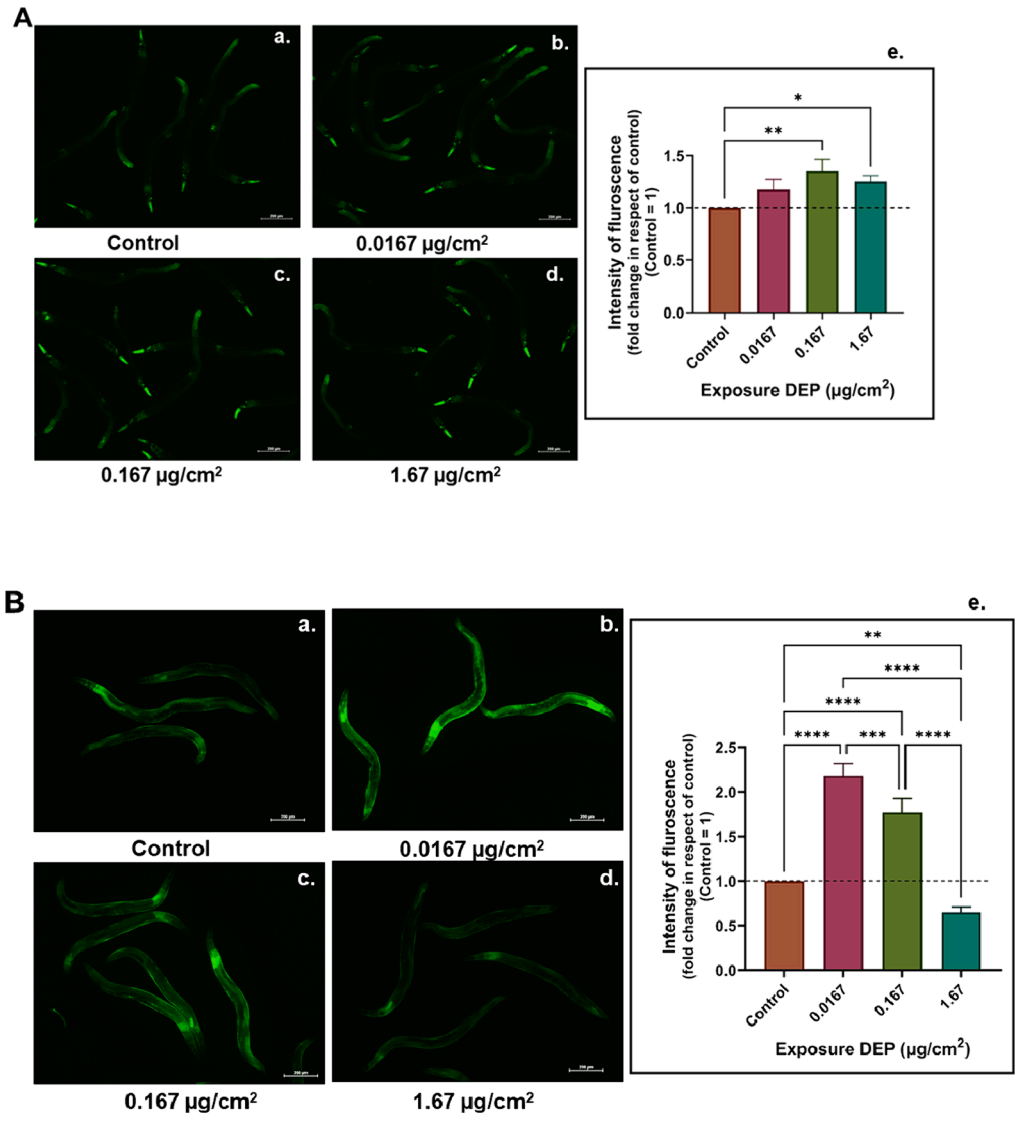

Fig. 6. Effects of DEP on induction of antioxidant enzyme expression. Exposures were conducted from bleached eggs until Day 4 on solid NGM plates, after which live worms were observed under a fluorescence microscope. Quantitative analysis of fluorescence intensity was performed using Image J software. **A.** Alterations in superoxide-dismutase (SOD-3) expressions in CF1553 strain, with the representative images of crawling path from reach exposure conditions – a. control, b. 0.0167 µg/cm^2, c. 0.167 µg/cm^2, d. 1.67 µg/cm^2, e. the graphical presentation of quantitative analysis fluorescence intensity in respect of control. **B.** Alterations in glutathione S-transferase (GST-4) expressions in CL2166 strain., with the representative images of the crawling path from reach exposure conditions – a. control, b. 0.0167 µg/cm^2, c. 0.167 µg/cm^2, d. 1.67 µg/cm^2, e. the graphical presentation of quantitative analysis fluorescence intensity in respect of control. Image scale bar 200 µm. Data are presented as Mean ± SD; * $p \leq 0.05$; ** $p \leq 0.005$; *** $p \leq 0.001$, **** $p < 0.0001$.

make the following considerations: most studies of toxicological characterization of particulate matter, including PM_{10}, $PM_{2.5}$, diesel, and nanomaterials, generally use concentrations in the range of 1–100 µg/mL and between 0.1 and 10 µg/cm^2 (Vilas-Boas et al., 2024). Theoretical models estimate that in bifurcations of the lower airways, where the highest doses of particles could be found, may be in the scope of the concentrations used in the present and other studies (Alfaro-Moreno et al., 2010), and the potential translocation from lungs into systemic targets are also within the studied range of concentrations (Quintana-Belmares et al., 2018a).

It is important to note a limitation in this study regarding establishing a direct connection between the analysed endpoints. However, we speculate on a clear link between antioxidant enzyme gene expression, neurodegeneration, and locomotion behaviour. The well-established association between oxidative stress and neurodegenerations is highlighted, with documented evidence of GST-4′s protective role in *C. elegans* against neurodegenerative diseases such as Parkinson's and Machado-Joseph disease (Pohl et al., 2019). Additionally, the RNAi knockdown of antioxidant enzyme genes (*sod-3*, *sod-4*, *ctl-3*) resulted in increased induction of intestinal ROS production and decreased locomotion in comparison to wild-type animals when exposed to fine $PM_{2.5}$ from coal combustion (Wu et al., 2017). In summary, the neuro-behavioural and developmental toxicity of DEP may stem from neuronal loss, neurotransmission abnormalities, and oxidative damage (Wang et al., 2023).

4. Conclusions

In summary, our findings support the detrimental impact of early-life and prolonged exposure to DEP, revealing a spectrum of adverse effects encompassing developmental delays, retarded growth, oxidative stress, and behavioural changes. Notably, we observed significant alterations in locomotion behaviour and crucial glutamatergic neurodegenerations, while DEP did not critically impact survival. The results of molecular

docking simulations suggested a higher affinity of the DEP compounds for the glutamatergic target than the dopaminergic one. Among the observed effects, oxidative stress and glutamatergic neurodegenerations are pivotal contributors to DEP-induced adverse outcomes, particularly influencing abnormal locomotion behaviour. These findings significantly contribute to our understanding of the potential association between DEP exposure and neurodegenerative diseases, shedding light on intricate mechanisms. The insights gained pave the way for future investigations into the specific neurodegenerative pathways induced by DEP.

CRediT authorship contribution statement

Nivedita Chatterjee: Conceptualization, investigation, methodology, data analysis, visualization and original draft writing. **Michael González-Durruthy:** In silico analysis, contributed to original draft writing. **Marta Daniela Costa:** Methodology, data analysis and visualization. **Ana R. Ribeiro:** Electron microscopic experiment and contributed to original draft writing. **Vânia Vilas-Boas:** Particles characterization and contributed to original draft writing. **Daniela Vilasboas-Campos:** Methodology and data analysis. **Patrícia Maciel:** Resources, supervision, and discussion. **Ernesto Alfaro-Moreno:** Conceptualization, resources, supervision, visualization, discussion and contributed to original draft writing. All authors contributed to the review of the manuscript.

Declaration of competing interest

The authors declare that they have no known competing financial interests or personal relationships that could have appeared to influence the work reported in this paper.

Data availability

Data will be made available on request.

Acknowledgement

This study was funded by the European Union's H2020 projects, Sinfonia (N.857253), LEARN (N.101057510) and iCare (N.101092971). The authors thank Dr. Tanima SenGupta for supporting the analysis of *C. elegans*' dopaminergic neuronal images. We also thank the Caenorhabditis Genetics Center (CGC), which is funded by NIH Office of Research Infrastructure Programs (P40 OD010440), for providing the C. elegans strains.

Appendix A. Supplementary material

Supplementary data to this article can be found online at https://doi.org/10.1016/j.envint.2024.108597.

References

Alfaro-Moreno, E.; Cm, G.-C.; De Vizcaya-Ruiz, A.; Rojas-Bracho, L.; Osornio-Vargas, A. Cellular Mechanisms behind Particulate Matter Air Pollution Related Health Effects. 2010.

Amador-Muñoz, O., Villalobos-Pietrini, R., Miranda, J., Vera-Avila, L.E., 2011. Organic compounds of PM2.5 in Mexico Valley: Spatial and temporal patterns, behavior and sources. Sci. Total Environ. 409, 1453–1465.

Armada-Moreira, A., Gomes, J.I., Pina, C.C., Savchak, O.K., Goncalves-Ribeiro, J., Rei, N., Pinto, S., Morais, T.P., Martins, R.S., Ribeiro, F.F., Sebastiao, A.M., Crunelli, V., Vaz, S.H., 2020. Going the extra (synaptic) mile: excitotoxicity as the road toward neurodegenerative diseases. Front Cell Neurosci. 14, 90.

Bargmann, C.I., Hartwieg, E., Horvitz, H.R., 1993. Odorant-selective genes and neurons mediate olfaction in C. elegans. Cell 74, 515–527.

Bolton, J.L., Huff, N.C., Smith, S.H., Mason, S.N., Foster, W.M., Auten, R.L., Bilbo, S.D., 2013. Maternal stress and effects of prenatal air pollution on offspring mental health outcomes in mice. Environ. Health Perspect. 121, 1075–1082.

Brenner, S., 1974. The genetics of Caenorhabditis elegans. Genetics 77, 71–94.

Caceres Quijano, M.F., de Paula Ribeiro, J., Josende, M.E., Santa-Helena, E., De Falco, A., Gioda, C.R., Gioda, A., 2022. Assessment of the effects of seasonality on the ecotoxicity induced by the particulate matter using the animal model Caenorhabditis elegans. Chemosphere 291, 132886.

Chung, M.-C., Tsai, M.-H., Que, D.E., Bongo, S.J., Hsu, W.-L., Tayo, L.L., Chao, H.-R., Lin, Y.-H., Lin, S.-L., Gou, Y.-Y., Hsu, Y.-C., Hou, W.-C., Huang, K.-L., 2019. Fine particulate matter-induced toxic effects in an animal model of caenorhabditis elegans. Aerosol Air Qual. Res. 19, 1068–1078.

Chung, M.-C., Huang, K.-L., Avelino, J.L., Tayo, L.L., Lin, C.-C., Tsai, M.-H., Lin, S.-L., Mansor, W.N.W., Su, C.-K., Huang, S.-T., 2020. Toxic assessment of heavily traffic-related fine particulate matter using an in-vivo wild-type caenorhabditis elegans model. Aerosol Air Qual. Res. 20, 1974–1986.

Collaborators, G.B.D.R.F., 2020. Global burden of 87 risk factors in 204 countries and territories, 1990-2019: a systematic analysis for the Global Burden of Disease Study 2019. Lancet (London, England) 396, 1223-1249.

Ema, M., Naya, M., Horimoto, M., Kato, H., 2013. Developmental toxicity of diesel exhaust: a review of studies in experimental animals. Reprod. Toxicol. (Elmsford, NY) 42, 1–17.

Felton, C.M., Johnson, C.M., 2014. Dopamine signaling in C. elegans is mediated in part by HLH-17-dependent regulation of extracellular dopamine levels. G3 (Bethesda) 4, 1081–1089. G3 (Bethesda.

Ficociello, G., Inverni, A., Massimi, L., Buccini, G., Canepari, S., Uccelletti, D., 2020. Assessment of the effects of atmospheric pollutants using the animal model Caenorhabditis elegans. Environ. Res. 191, 110209.

Fuller, R., Landrigan, P.J., Balakrishnan, K., Bathan, G., Bose-O'Reilly, S., Brauer, M., Caravanos, J., Chiles, T., Cohen, A., Corra, L., Cropper, M., Ferraro, G., Hanna, J., Hanrahan, D., Hu, H., Hunter, D., Janata, G., Kupka, R., Lanphear, B., Lichtveld, M., Martin, K., Mustapha, A., Sanchez-Triana, E., Sandilya, K., Schaefli, L., Shaw, J., Seddon, J., Suk, W., Téllez-Rojo, M.M., Yan, C., 2022. Pollution and health: a progress update. Lancet Planet. Health 6, e535–e547.

Garcia Manriquez, B.A., Papapanagiotou, J.A., Strysick, C.A., Green, E.H., Kikis, E.A., 2023. Nanoparticulate air pollution disrupts proteostasis in Caenorhabditis elegans. PLoS One 18, e0275137.

Griffin, E.F., Yan, X., Caldwell, K.A., Caldwell, G.A., 2018. Distinct functional roles of Vps41-mediated neuroprotection in Alzheimer's and Parkinson's disease models of neurodegeneration. Hum Mol Genet 27, 4176–4193.

Griffin, E.F., Scopel, S.E., Stephen, C.A., Holzhauer, A.C., Vaji, M.A., Tuckey, R.A., Berkowitz, L.A., Caldwell, K.A., Caldwell, G.A., 2019. ApoE-associated modulation of neuroprotection from Abeta-mediated neurodegeneration in transgenic Caenorhabditis elegans. Dis. Model Mech. 12, dmm037218.

Guo, X., Bian, P., Liang, J., Wang, Y., Li, L., Wang, J., Yuan, H., Chen, S., Xu, A., Wu, L., 2014. Synergistic effects induced by a low dose of diesel particulate extract and ultraviolet-A in Caenorhabditis elegans: DNA damage-triggered germ cell apoptosis. Chem Res Toxicol 27, 990–1001.

Guseynov, A.D., Pisarev, S.A., Shulga, D.A., Palyulin, V.A., Fedorov, M.V., Karlov, D.S., 2019. Computational characterization of the glutamate receptor antagonist perampanel and its close analogs: density functional exploration of conformational space and molecular docking study. J. Mol. Model. 25, 312.

Haghani, A., Dalton, H.M., Safi, N., Shirmohammadi, F., Sioutas, C., Morgan, T.E., Finch, C.E., Curran, S.P., 2019. Air pollution alters caenorhabditis elegans development and lifespan: responses to traffic-related nanoparticulate matter. J. Gerontol. A Biol. Sci. Med. Sci. 74, 1189–1197.

Hannah Ritchie, Roser, Max, 2022. "Outdoor Air Pollution" Published online at OurWorldInData.org. <https://ourworldindata.org/outdoor-air-pollution> [Online Resource].

Hughes, S., van Dop, M., Kolsters, N., van de Klashorst, D., Pogosova, A., Rijs, A.M., 2022. Using a Caenorhabditis elegans Parkinson's Disease Model to Assess Disease Progression and Therapy Efficiency. Pharmaceuticals (Basel, Switzerland) 15.

Jain, S., Sharma, S.K., Vijayan, N., Mandal, T.K., 2020. Seasonal characteristics of aerosols (PM(2.5) and PM(10)) and their source apportionment using PMF: a four year study over Delhi, India. In: Environ. Pollut. (Barking, Essex : 1987), p. 114337.

Kaletta, T., Hengartner, M.O., 2006. Finding function in novel targets: C. elegans as a model organism. Nat. Rev. Drug Discov. 5, 387–398.

Krzyzanowski, B., Searles Nielsen, S., Turner, J.R., Racette, B.A., 2023. Fine particulate matter and parkinson disease risk among medicare beneficiaries. Neurology 101, e2058–e2067.

Leung, M.C., Williams, P.L., Benedetto, A., Au, C., Helmcke, K.J., Aschner, M., Meyer, J. N., 2008. Caenorhabditis elegans: an emerging model in biomedical and environmental toxicology. Toxicol. Sci.: Off. J. Soc. Toxicol. 106, 5–28.

Li, B., Ma, Y., Zhou, Y., Chai, E., 2023. Research progress of different components of PM (2.5) and ischemic stroke. Sci. Rep. 13, 15965.

Li, P., Xu, T., Wu, S., Lei, L., He, D., 2017. Chronic exposure to graphene-based nanomaterials induces behavioral deficits and neural damage in Caenorhabditis elegans. J. Appl. Toxicol. 37, 1140–1150.

Limke, A., Scharpf, I., Blesing, F., von Mikecz, A., 2023. Tire components, age and temperature accelerate neurodegeneration in C. elegans models of Alzheimer's and Parkinson's disease. In: Environ. Pollut. (Barking, Essex : 1987), p. 121660.

Liu, X., Ge, P., Lu, Z., Cao, M., Chen, W., Yan, Z., Chen, M., Wang, J., 2023. Ecotoxicity induced by total, water soluble and insoluble components of atmospheric fine particulate matter exposure in Caenorhabditis elegans. Chemosphere 316, 137672.

Mano, I., Straud, S., Driscoll, M., 2007. Caenorhabditis elegans glutamate transporters influence synaptic function and behavior at sites distant from the synapse. J. Biol. Chem. 282, 34412–34419.

Markovich, Z.R., Hartman, J.H., Ryde, I.T., Hershberger, K.A., Joyce, A.S., Ferguson, P. L., Meyer, J.N., 2022. Mild pentachlorophenol-mediated uncoupling of mitochondria

depletes ATP but does not cause an oxidized redox state or dopaminergic neurodegeneration in Caenorhabditis elegans. Curr Res Toxicol 3, 100084.
Nussbaum-Krammer, C.I., Neto, M.F., Brielmann, R.M., Pedersen, J.S., Morimoto, R.I., 2015. Investigating the spreading and toxicity of prion-like proteins using the metazoan model organism C. elegans. J. Visual. Exp.: JoVE 52321.
Olasehinde, T.A., Olaniran, A.O., 2022. Neurotoxicity of polycyclic aromatic hydrocarbons: a systematic mapping and review of neuropathological mechanisms. Toxics 10, 417.
Park, M., Joo, H.S., Lee, K., Jang, M., Kim, S.D., Kim, I., Borlaza, L.J.S., Lim, H., Shin, H., Chung, K.H., Choi, Y.-H., Park, S.G., Bae, M.-S., Lee, J., Song, H., Park, K., 2018. Differential toxicities of fine particulate matters from various sources. Sci. Rep. 8, 17007.
Peters, A., 2023. Ambient air pollution and Alzheimer's disease: the role of the composition of fine particles. Proc. Natl. Acad. Sci. 120.
Piggott, B.J., Liu, J., Feng, Z., Wescott, S.A., Xu, X.Z., 2011. The neural circuits and synaptic mechanisms underlying motor initiation in C. elegans. Cell 147, 922–933.
Pohl, F., Teixeira-Castro, A., Costa, M.D., Lindsay, V., Fiuza-Fernandes, J., Goua, M., Bermano, G., Russell, W., Maciel, P., Lin, K.T., P., 2019. GST-4-dependent suppression of neurodegeneration in C. elegans models of parkinson's and machado-joseph disease by rapeseed pomace extract supplementation. Front. Neurosci. 13, 1091.
Quintana-Belmares, R., Hernández-Pérez, G., Montiel-Dávalos, A., Gustafsson, Å., Miranda, J., Rosas-Pérez, I., López-Marure, R., Alfaro-Moreno, E., 2018a. Urban particulate matter induces the expression of receptors for early and late adhesion molecules on human monocytes. Environ. Res. 167, 283–291.
Quintana-Belmares, R.O., Krais, A.M., Esfahani, B.K., Rosas-Pérez, I., Mucs, D., López-Marure, R., Bergman, Å., Alfaro-Moreno, E., 2018b. Phthalate esters on urban airborne particles: levels in PM10 and PM2.5 from Mexico City and theoretical assessment of lung exposure. Environ. Res. 161, 439–445.
Singh, B.P., Singh, D., Kumar, K., Jain, V.K., 2021. Study of seasonal variation of PM2.5 concentration associated with meteorological parameters at residential sites in Delhi, India. J. Atmos. Chem. 78, 161–176.
Smith, L.L., Ryde, I.T., Hartman, J.H., Romersi, R.F., Markovich, Z., Meyer, J.N., 2019. Strengths and limitations of morphological and behavioral analyses in detecting dopaminergic deficiency in Caenorhabditis elegans. Neurotoxicology 74, 209–220.
Soares, M.V., Charao, M.F., Jacques, M.T., Dos Santos, A.L.A., Luchese, C., Pinton, S., Avila, D.S., 2020. Airborne toluene exposure causes germline apoptosis and neuronal damage that promotes neurobehavioural changes in Caenorhabditis elegans. Environ. Pollut. (Barking, Essex: 1987) (256), 113406.
Sun, L., Lin, Z., Liao, K., Xi, Z., Wang, D., 2015. Adverse effects of coal combustion related fine particulate matter (PM2.5) on nematode Caenorhabditis elegans. Sci. Total Environ. 512–513, 251–260.
Suzuki, T., Oshio, S., Iwata, M., Saburi, H., Odagiri, T., Udagawa, T., Sugawara, I., Umezawa, M., Takeda, K., 2010. In utero exposure to a low concentration of diesel exhaust affects spontaneous locomotor activity and monoaminergic system in male mice. Part. Fibre Toxicol. 7, 7.
Thirtamara Rajamani, K., Doherty-Lyons, S., Bolden, C., Willis, D., Hoffman, C., Zelikoff, J., Chen, L.C., Gu, H., 2013. Prenatal and early-life exposure to high-level diesel exhaust particles leads to increased locomotor activity and repetitive behaviors in mice. Autism Res.: Off. J. Int. Soc. Autism Res. 6, 248–257.
Van Den Broucke, S., Vanoirbeek, J., Alfaro-Moreno, E., Hoet, P., 2020. Contribution of mast cells in irritant-induced airway epithelial barrier impairment in vitro. Toxicol. Ind. Health 36, 823–834.
Vilasboas-Campos, D., Costa, M.D., Teixeira-Castro, A., Rios, R., Silva, F.G., Bessa, C., Dias, A.C.P., Maciel, P., 2021. Neurotherapeutic effect of Hyptis spp. leaf extracts in Caenorhabditis elegans models of tauopathy and polyglutamine disease: role of the glutathione redox cycle. Free Rad. Biol. Med. 162, 202–215.
von Mikecz, A., Schikowski, T., 2020. Effects of airborne nanoparticles on the nervous system: amyloid protein aggregation, neurodegeneration and neurodegenerative diseases. Nanomaterials (basel, Switzerland) 10, 1349.
Wang, Y., Gai, T., Zhang, L., Chen, L., Wang, S., Ye, T., Zhang, W., 2023. Neurotoxicity of bisphenol A exposure on Caenorhabditis elegans induced by disturbance of neurotransmitter and oxidative damage. Ecotoxicol. Environ. Saf. 252, 114617.
Wang, M., Nie, Y., Liu, Y., Dai, H., Wang, J., Si, B., Yang, Z., Cheng, L., Liu, Y., Chen, S., Xu, A., 2019. Transgenerational effects of diesel particulate matter on Caenorhabditis elegans through maternal and multigenerational exposure. Ecotoxicol. Environ. Saf. 170, 635–643.
Wichmann, H.E., 2007. Diesel exhaust particles. Inhal. Toxicol. 19 (Suppl 1), 241–244.
Vilas-Boas, V., Chatterjee, N., Carvalho A, Alfaro-Moreno, E., 2024. Preprints. https://doi.org/10.20944/preprints202404.0131.v1.
World Health Organization, (ed). WHO Global Air Quality Guidelines: Particulate Matter (PM2.5 and PM10), Ozone, Nitrogen Dioxide, Sulfur Dioxide and Carbon Monoxide. 2021.
Wu, Q., Han, X., Wang, D., Zhao, F., Wang, D., 2017. Coal combustion related fine particulate matter (PM(2.5)) induces toxicity in Caenorhabditis elegans by dysregulating microRNA expression. Toxicol. Res. 6, 432–441.
Xiong, H., Pears, C., Woollard, A., 2017. An enhanced C. elegans based platform for toxicity assessment. Sci. Rep. 7, 9839.
Yan, C., Wu, X., Cao, X., Li, M., Zhou, L., Xiu, G., Zeng, J., 2021. In vitro and in vitro toxicity study of diesel exhaust particles using BEAS-2B cell line and the nematode Caenorhabditis elegans as biological models. Environ. Sci. Pollut. Res. Int. 28, 60704–60716.
Yang, R., Ge, P., Liu, X., Chen, W., Yan, Z., Chen, M., 2023. Chemical composition and transgenerational effects on caenorhabditis elegans of seasonal fine particulate matter. Toxics 11.
Yu, Y., Hua, X., Chen, H., Wang, Z., Han, Y., Chen, X., Yang, Y., Xiang, M., 2022. Glutamatergic transmission associated with locomotion-related neurotoxicity to lindane over generations in Caenorhabditis elegans. Chemosphere 290, 133360.
Zhang, W., Li, Z., Li, G., Kong, L., Jing, H., Zhang, N., Ning, J., Gao, S., Zhang, Y., Wang, X., Tao, J., 2023. PM(2.5) induce lifespan reduction, insulin/IGF-1 signaling pathway disruption and lipid metabolism disorder in Caenorhabditis elegans. Front. Public health 11, 1055175.
Zhao, Y., Lin, Z., Jia, R., Li, G., Xi, Z., Wang, D., 2014. Transgenerational effects of traffic-related fine particulate matter (PM(2). (5)) on nematode Caenorhabditis elegans. J. Hazard. Mater. 274, 106–114.
Zhao, Y., Jin, L., Chi, Y., Yang, J., Zhen, Q., Wu, H., 2019. Fine particulate matter leads to unfolded protein response and shortened lifespan by inducing oxidative stress in C. elegans. Oxid. Med. Cell Longev. 2019.
Zheng, M., Salmon, L.G., Schauer, J.J., Zeng, L., Kiang, C.S., Zhang, Y., Cass, G.R., 2005. Seasonal trends in PM2.5 source contributions in Beijing, China. Atmos. Environ. 39, 3967–3976.